Active Rheology in Odd Viscosity Systems

C. J. O. REICHHARDT AND C. REICHHARDT

Theoretical Division and Center for Nonlinear Studies, Los Alamos National Laboratory, Los Alamos, New Mexico 87545, USA

Abstract – Odd viscosity arises in systems with time non-dissipative effects. One method to probe changes a single probe particle driven though a medium, a ter that active rheology in a system with odd viscosity ar novel effects, including a speed up of the probe particle background medium creates a velocity boost of the docontrast, the probe particle velocity in the dissipation with increasing system density. We also show that the probe particle, and that both the Hall angle and the variable These results should be general to other systems with magnets.

Introduction. – Viscosity in fluids or glasses is associated with dissipation, and an increase in density generally produces an increase of viscosity. For example, when a glass transition is approached from below by increasing the density, the viscosity increases [1]. An effective method for examining changes in the viscosity of a medium is active Abstract - Odd viscosity arises in systems with time reversal symmetry breaking, which creates non-dissipative effects. One method to probe changes in viscosity is to examine the dynamics of a single probe particle driven though a medium, a technique known as active rheology. We show that active rheology in a system with odd viscosity and no quenched disorder reveals a variety of novel effects, including a speed up of the probe particle with increasing system density when the background medium creates a velocity boost of the driven particle due to the Magnus effect. In contrast, the probe particle velocity in the dissipation-dominated limit monotonically decreases with increasing system density. We also show that the odd viscosity imparts a Hall angle to the probe particle, and that both the Hall angle and the velocity boost depend strongly on the drive. These results should be general to other systems with odd viscosity, including skyrmions in chiral

examining changes in the viscosity of a medium is active rheology, where the drag or fluctuations on a single probe particle are measured as the particle is pushed through the medium while the density or driving force is varied [2–6]. Active rheology has been used to study viscosity changes Active rheology has been used to study viscosity changes in systems undergoing glass [2,4,5,7–9] or jamming [10–12] transitions. The probe particle velocity decreases or even drops to zero at a pinning transition when the driving force drops below a critical value or the density rises above a \sim critical value [2, 5, 10, 13–15]. The corresponding viscosity increase is produced by the increased interactions with the background particles, since the probe particle must push more particles out of its way in order to translate in the driving direction. Active rheology has also been used to study viscous properties in active matter systems [16], depletion interactions [17], local melting [18], and complex soft matter systems [19, 20]

In systems where time reversal symmetry breaking occurs, another type of viscosity termed odd viscosity can arise. Here, the Onsager reciprocal relations break down, there are no energy eigenstates, and nondissipative effects can arise due to the leaking of energy from one mode to another. Odd viscosity is also called gyroviscosity since it can appear in systems with gyroscopic effects such as charged particles in magnetic fields, quantum Hall fluids [21, 22], plasmas [23], fluid vortices [24], and non-dissipative systems with broken parity [25]. More recently, odd viscosity has been studied in chiral active matter systems or active spinners [26–30] where it generates flows that are perpendicular to pressure [26], unidirectional propagation of edge modes [27], topological waves [28], and anomalous flows [31]. Recently, similar effects have also been explored in systems that have odd elasticity [32] or exhibit non-reciprocal phase transitions [33, 34].

Here we show that odd viscosity can have pronounced effects on active rheology, producing significantly different and even reversed behavior compared to that found in systems with only dissipative viscosity. One of the most prominent distinctions is that the velocity of the probe particle at a constant drive can increase with increasing system density, which is the opposite of what is observed in systems with dissipative viscosity. Another consequence is that the probe particle exhibits a finite Hall angle with a value that depends on the driving force and the density. A speed up effect appears as a function of increasing density when a density gradient is built up by the finite Hall angle motion of the probe particle. The odd viscosity transfers the pressure from the unbalanced density gradient forces into a flow perpendicular to these forces and parallel to the driving direction. The speed up effect has a non-monotonic dependence on the driving force and pro-

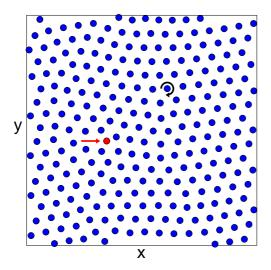


Fig. 1: (a) Image of a portion of the sample at density $\rho=0.2$. The red particle is being driven in the x-direction (red arrow) at a constant force F_D , and it interacts with the surrounding bath particles (blue). The black arrow around a representative bath particle indicates the direction of chirality of the Magnus term

duces velocity-force signatures distinct from those found in the overdamped limit. The specific model we consider represents skyrmions in chiral magnets [35–37] which have a strong Magnus force component due to their topology [37–39]. Our results indicate that skyrmions are another system that exhibits strong odd-viscosity effects, and our findings should be general to the broader class of systems with odd viscosity.

Simulation and System. — In Fig. 1 we show a snapshot of a portion of our two-dimensional system, which has periodic boundary conditions in the x and y directions. A probe particle is subjected to a constant driving force of $\mathbf{F}_D = F_D \hat{\mathbf{x}}$ and interacts with a bath of other particles which experience both dissipative and Magnus forces. The chirality of the Magnus force is indicated by the circulating arrow around a representative bath particle. The dynamics of particle i obey the following equation of motion:

$$\alpha_d \mathbf{v}_i + \alpha_m \mathbf{\hat{z}} \times \mathbf{v}_i = \mathbf{F}_i^{ss} + \mathbf{F}^D \tag{1}$$

Here \mathbf{v}_i (\mathbf{r}_i) is the velocity (position) of particle i. The dissipative damping constant α_d aligns the velocity in the direction of the net applied forces, while the Magnus term α_m creates a velocity component perpendicular to the net forces and produces the odd-viscosity behavior. The Magnus term can arise from spinning of the particles, cyclotron motion, or the intrinsic topological nature of the particle as in the case of magnetic skyrmions [37,38]. The particle-particle interaction force is $\mathbf{F}_i^{ss} = \sum_{j=1}^N K_1(r_{ij})\hat{\mathbf{r}}_{ij}$ where $r_{ij} = |\mathbf{r}_i - \mathbf{r}_j|$, $\hat{\mathbf{r}}_{ij} = (\mathbf{r}_i - \mathbf{r}_j)/r_{ij}$, and K_1 is the modified Bessel function which gives a smoothly decreasing force of the form e^r/r to create an intermediate range repulsive interaction. This interaction has been used previously

to model skyrmions in chiral magnets [40]; however, the smooth repulsive interaction should also be relevant for other systems with spinning objects or some form of Magnus force, including spinning magnetic or charged colloids, fluid vortices, fractors, Wigner crystals in a magnetic field, or certain types of chiral active matter. The driving force $\mathbf{F}_D = F_D \hat{\mathbf{x}}$ is applied only to the probe particle. We measure the probe particle velocity parallel, $\langle V_{||} \rangle$, and perpendicular, $\langle V_{\perp} \rangle$ to the drive, where the average is taken over time, as well as the net velocity $|V| = (\langle V_{\perp} \rangle^2 + \langle V_{||} \rangle^2)^{1/2}$. In the absence of any collisions, the probe particle has an intrinsic Hall angle of $\theta_{\text{Hall}}^{\text{int}} = -\arctan(\alpha_m/\alpha_d)$, while in the presence of the background particles, we measure the actual Hall angle $\theta_{\text{Hall}} = \arctan(\langle V_{\perp} \rangle / \langle V_{||} \rangle)$. In the damping-dominated limit of $\alpha_m = 0$, $\theta_{\text{Hall}}^{\text{int}} = 0^{\circ}$. In skyrmion systems this is referred to as the skyrmion Hall angle [37–39] and it has been observed directly in experiment [41-45].

Results— We first consider a constant driving force of $F_D=1.0$ for varied system density ρ . In order to more easily compare systems with different ratios of damping to Magnus forces, we impose the constraint $\alpha_m^2 + \alpha_d^2 = 1.0$. In the single particle limit, $|V| = F_D/(\alpha_m^2 + \alpha_d^2)^{1/2}$, which under our constraint gives $|V| = F_D$, independent of the ratio of the force terms. This makes it easy to determine whether the velocity is decreased or boosted with respect to the single particle limit as we change ρ .

In Fig. 2(a) we plot |V| versus ρ for an overdamped system with $\alpha_m=0$ and a Magnus dominated system with $\alpha_m/\alpha_d=4.9246$. In the overdamped limit, |V| monotonically decreases with increasing ρ since the probe particle must displace a larger number of particles in order to move through the system. Here |V| is always lower than the value $|V|=F_D=1.0$ expected in the single particle limit. In contrast, for the Magnus dominated system |V| has the opposite behavior and increases with increasing density before reaching a maximum value near $\rho=0.8$. As ρ increases further, |V| gradually decreases. Although |V|=1 for low ρ , it rises above this value over an extended range of density. At $\rho=0.8$, |V| for the Magnus dominated system is about three times higher than |V| in the overdamped system.

In Fig. 2(b) we plot $\langle V_{||} \rangle$ and $\langle V_{\perp} \rangle$ for the $\alpha_m/\alpha_d=4.9246$ sample. In the single particle limit, $|\langle V_{\perp} \rangle|=4.9246\langle V_{||} \rangle$. As the density ρ of the bath particles increases, $\langle V_{||} \rangle$ increases to a maximum value near $\rho=2.0$, while the magnitude of $\langle V_{\perp} \rangle$ reaches its largest value near $\rho=0.8$. Both quantities decrease as ρ increases further. For the overdamped case (not shown), $\langle V_{\perp} \rangle=0$ and $\langle V_{||} \rangle$ is identical to |V|. In Fig. 2(c) we plot the Hall angle $\theta_{\rm Hall}$ versus ρ . In the overdamped limit, $\theta_{\rm Hall}=0^{\circ}$ for all ρ . For the Magnus dominated system, in the single particle limit we would expect to obtain $\theta_{\rm Hall}=-\arctan(\alpha_m/\alpha_d)=-78.52^{\circ}$, but when interactions with the bath particles are present, the magnitude of $\theta_{\rm Hall}$ monotonically decreases with increasing ρ and reaches a value close to zero for $\rho>3.0$.

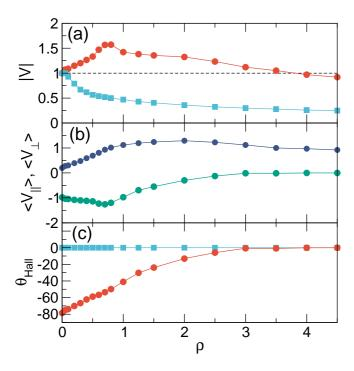


Fig. 2: (a) The total probe particle velocity |V| versus density ρ for a system with $F_D=1.0$ in the overdamped regime with $\alpha_m=0$ (blue squares) and in the Magnus dominated regime with $\alpha_m/\alpha_d=4.9246$ (red circles). The dashed black line is the expected velocity in the single particle limit. (b) The velocities parallel and perpendicular to the drive, $\langle V_{||} \rangle$ (blue) and $\langle V_{\perp} \rangle$ (green), versus ρ for the Magnus dominated system in panel (a). (c) The corresponding measured skyrmion Hall angle $\theta_{\rm Hall}$ versus ρ for the overdamped system (blue squares) and the Magnus dominated system (red circles).

In Fig. 3(a) we plot |V| versus ρ for the system in Fig. 2 with $F_D = 1.0$ at $\alpha_m/\alpha_d = 0.0, 0.1, 0.204, 0.3145, 0.4364,$ 0.577, 0.75, 1.0, 1.33, 2.0647, 3.0424, 4.9246, 9.95, and 19.97, as well as for a system with $\alpha_d = 0.0$ and $\alpha_m = 1.0$. When $\alpha_m/\alpha_d < 0.75$, |V| decreases monotonically with increasing ρ and always falls below the single particle limit of $V_0 = 1.0$, indicated by a dashed line. For $\alpha_m/\alpha_d > 0.75$, there is a growing window with $|V| > V_0$ indicating a velocity boost. At lower ρ , |V| increases with increasing ρ ; however, at higher ρ , |V| drops below V_0 . For $\rho = 0$ all of the curves start at the single particle value of $|V| = V_0$, indicating that the velocity boosts are the result of collective interaction effects. For the systems with the largest Magnus terms, the window of increasing |V| extends as high as $\rho = 4.0$. Figure 3(b) shows the corresponding θ_{Hall} versus ρ . With increasing ρ , the magnitude of θ_{Hall} monotonically decreases from its value in the single particle limit, indicting that the increase in collision frequency is responsible for the reduction of the Hall angle. There is an extended region where $\theta_{\rm Hall}$ is close to zero at the higher densities.

In Fig. 4(a) we plot |V| versus F_D for systems with $\rho = 0.8$ at $\alpha_m/\alpha_d = 0.0, 1.0, 2.0647, 4.9245, and 19.97,$

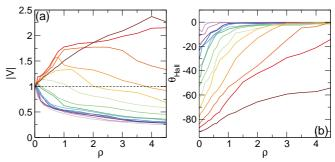


Fig. 3: (a) |V| versus ρ for the system in Fig. 2 with $F_D=1.0$ at $\alpha_m/\alpha_d=0.0,\ 0.1,\ 0.204,\ 0.3145,\ 0.4364,\ 0.577,\ 0.75,\ 1.0,\ 1.33,\ 2.0647,\ 3.0424,\ 4.9246,\ 9.95,\ and\ 19.97,\ from bottom to second from top, where the brown curve is for a system with <math>\alpha_d=0.0$ and $\alpha_m=1.0$. The dashed line is the single particle limit of $V_0=F_D=1.0$. (c) $\theta_{\rm Hall}$ versus ρ for the same system.

and for a system with $\alpha_d = 0.0$ and $\alpha_m = 1.0$. When $\alpha_m/\alpha_d < 2.064$, |V| falls below the single particle limit, while for $\alpha_m/\alpha_d \geq 2.064$, a portion of the velocity curve rises above the single particle limit, indicating a boost effect. In Fig. 4(b) we quantify the boost by plotting $\Delta V = |V|/V_0$ versus F_D , where V_0 is the velocity in the single particle limit. At low drives ΔV < 1.0, indicating increased damping due to the particle-particle interactions. In fact, the probe particle is pinned and unable to move through the background particles for $F_D < 0.15$. For $\alpha_m/\alpha_d < 2.064$, ΔV gradually approaches $\Delta V = 1.0$ with increasing drive, while for $\alpha_m/\alpha_d > 2.064$, ΔV passes through a maximum and then decreases back toward $\Delta V = 1.0$ as F_D increases. For $\alpha_m/\alpha_d = 19.97$, the maximum boost is close to 1.75 times higher than the velocity in the single particle limit. In Fig. 4(c) we plot the corresponding θ_{Hall} versus F_D showing that θ_{Hall} monotonically increases with increasing velocity and approaches the single particle limit at large drives. The drive dependence of the Hall angle is similar to what has been observed for skyrmions moving over quenched disorder, where the skyrmion Hall angle is zero near the depinning transition and increases with increasing skyrmion velocity up to its intrinsic value [39,41–46]. In our case there is no quenched disorder, but scattering occurs during the collisions with other particles. For active rheology in an overdamped system, the probe particle velocity is always lower than the single particle limit [2].

The origin of the dependence of the velocity on ρ and F_D is the attempts of the probe particle to move along its intrinsic Hall angle $\theta_{\rm Hall}^{\rm int} = -\arctan(\alpha_m/\alpha_d)$. The resulting collisions with the background particles produce a density build up of $\Delta \rho$ below the probe particle, perpendicular to the drive direction. Due to the repulsive nature of the particle-particle interactions, the probe particle experiences an unbalanced force in the positive y-direction from the background particles. Since the Magnus force or the odd viscosity creates a velocity component perpendic-

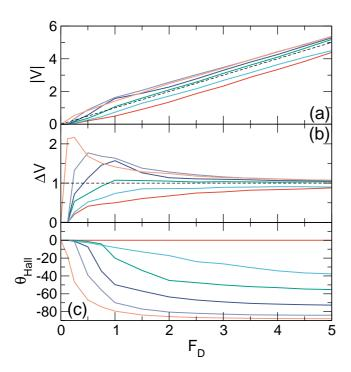


Fig. 4: (a) |V| versus F_D for systems with $\rho=0.8$ and $\alpha_m/\alpha_d=0.0$ (red), 1.0 (light blue), 2.0647 (green), 4.9245 (dark blue), and 19.97 (light purple), with the orange curve indicating a system with $\alpha_d=0$ and $\alpha_m=1.0$. The dashed line is the curve for the single particle limit. (b) The corresponding velocity boost $\Delta V=|V|/V_0$ versus F_D , where V_0 is the velocity in the single particle limit. (c) The corresponding $\theta_{\rm Hall}$ versus F_D .

ular to the net force, the probe exhibits enhanced velocity in the positive x direction, parallel to the drive, of magnitude $V_x \propto F_D \alpha_d + \alpha_m \Delta \rho$. As α_m increases, the boost increases. The local density inhomogeneity also causes the probe particle to move at an angle less than $\theta_{\text{Hall}}^{\text{int}}$. The magnitude of $\Delta \rho$ depends on the overall particle density. At large ρ , it is difficult to maintain a local disturbance in the background particle density, reducing $\Delta \rho$ and reducing the boost, as shown in Fig. 3(a). At low F_D , the probe particle is moving slowly enough that the surrounding particles have time to relax away the local gradient, so $\Delta \rho$ is close to zero and the boost is small, while when the probe particle is moving rapidly at high F_D , the surrounding particles do not have time to form a local density gradient and $\Delta \rho$ is again small, giving a reduced boost at high velocities, as shown in Fig. 4(b). Velocity boosts due to the Magnus force have been observed for skyrmions interacting with a repulsive defect line or edge barrier, where the force from the barrier is perpendicular to the driving force but gets converted by the Magnus term into a velocity component in the driving direction [47,48]. In previous work on a probe particle moving in an overdamped system where the particles are subjected to chiral ac driving, the probe exhibited a drive dependent Hall angle, but there was no velocity boost [49].

We next relax the constraint $\alpha_m^2 + \alpha_d^2 = 1.0$ and hold

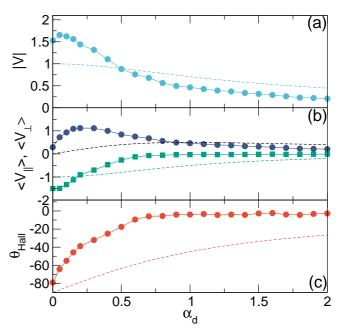


Fig. 5: (a) |V| versus α_d for a system with $F_D=1.0$ and $\alpha_m=1.0$ at $\rho=1.0$ (blue circles) and the single particle limit of $|V|=F_D/(1+\alpha_d^2)^{1/2}$ (dashed line). (b) The corresponding $\langle V_{||} \rangle$ (blue circles) and $\langle V_{\perp} \rangle$ (green squares). The single particle limits are $\langle V_{||} \rangle = F_D \alpha_d/(1+\alpha_d^2)$ (black dashed line) and $\langle V_{\perp} \rangle = -F_D/(1+\alpha_d^2)$ (green dashed line). (c) $\theta_{\rm Hall} = \arctan(\langle V_{\perp} \rangle/\langle V_{||} \rangle)$ at $\rho=1.0$ (red circles) and the single particle limit of $\theta_{\rm Hall}=-\arctan(1/\alpha_d)$ (dashed line).

 α_m fixed while varying α_d over the range 0.0 to 2.0. Here, in the single particle limit, $|V| = F_D/(\alpha_m^2 + \alpha_d^2)^{1/2}$, $\langle V_{||} \rangle = F_D \alpha_d/(\alpha_m^2 + \alpha_d^2)$, and $\langle V_{\perp} \rangle = -F_D \alpha_m/(\alpha_m^2 + \alpha_d^2)$. In Fig. 5(a) we plot |V| versus α_d for a system with $\alpha_m = 1.0$ and $F_D = 1.0$ at $\rho = 1.0$. The velocity is boosted above the single particle limit for $\alpha_d < 0.5$, while for higher values of α_d , |V| drops below the single particle limit, indicating increased damping. Figure 5(b) shows $\langle V_{||} \rangle$ and $\langle V_{\perp} \rangle$ versus α_d for the $\rho = 1.0$ system. The magnitudes of the velocities in both directions are first boosted above the single particle limit, and then drop below the single particle limit at larger α_d . In Fig. 5(c) we plot the corresponding $\theta_{\text{Hall}} = \arctan(\langle V_{\perp} \rangle / \langle V_{||} \rangle)$ versus α_d for the system in Fig. 5(b) along with the single particle limit of $\theta_{\text{Hall}} = -\arctan(\alpha_m/\alpha_d) = -\arctan(1/\alpha_d)$. The magnitude of the Hall angle is reduced in the interacting system, and approaches zero at the crossover near $\alpha_d = 0.5$ from the regime of boosted velocities to the damped regime.

In summary, we have examined the active rheology of a single probe particle driven though a medium with odd viscosity in the absence of quenched disorder. We find striking differences in the behavior of the drag and velocity-force relations compared to what is observed for active rheology in overdamped systems. When the driving force is fixed, we show that if the odd viscosity is sufficiently large, the velocity of the particle can actu-

ally increase as the density of the background particles increases, while in the overdamped regime the opposite effect is observed and the velocity monotonically decreases with increasing density due to the increased frequency of particle-particle collisions. The velocity-force curves for the odd viscosity system show regimes in which the velocity is boosted to a value significantly higher than what is observed in the single particle limit. This velocity boost, which reaches a maximum value at a specific driving force, arises due to the formation of a local density gradient around the driven particle, which produces unbalanced repulsive forces perpendicular to the driving direction that are converted by the Magnus term into a velocity component parallel to the driving direction. At low and high drives, the size of these density gradients and the corresponding velocity boost are strongly reduced. The probe particle also exhibits a finite Hall angle which depends on density and driving force. The Hall angle increases from zero at low drives and approaches the single particle limit at higher drives, similar to the behavior observed for skyrmions driven over quenched disorder. Our results should be general to a wide class of systems with odd viscosity, including skyrmions in chiral magnets.

* * *

We gratefully acknowledge the support of the U.S. Department of Energy through the LANL/LDRD program for this work. This work was supported by the US Department of Energy through the Los Alamos National Laboratory. Los Alamos National Laboratory is operated by Triad National Security, LLC, for the National Nuclear Security Administration of the U. S. Department of Energy (Contract No. 892333218NCA000001).

REFERENCES

- MAURO J. C., YUE Y., ELLISON A. J., GUPTA P. K. and ALLAN D. C., Proc. Natl. Acad. Sci. (USA), 106 (2009) 10780
- [2] Habdas P., Schaar D., Levitt A. C. and Weeks
 E. R., Europhys. Lett., 67 (2004) 477.
- [3] SQUIRES T. M. and BRADY J. F., Phys. Fluids, 17 (2005) 073101.
- [4] WILSON L. G. and POON W. C. K., Phys. Chem. Chem. Phys., 13 (2011) 10617.
- [5] VOIGTMANN T. and FUCHS M., Eur. Phys. J. Spec. Top., 222 (2013) 2819.
- [6] ZIA R. N., Ann. Rev. Fluid Mech., 50 (2018) 371.
- [7] GAZUZ I., PUERTAS A. M., VOIGTMANN T. and FUCHS M., Phys. Rev. Lett., 102 (2009) 248302.
- [8] WINTER D., HORBACH J., VIRNAU P. and BINDER K., Phys. Rev. Lett., 108 (2012) 028303.
- [9] Yu J. W., Rahbari S. H. E., Kawasaki T., Park H. and Lee W. B., $Sci.\ Adv.,\ {\bf 6}\ (2020)$.
- [10] DROCCO J. A., HASTINGS M. B., REICHHARDT C. J. O. and REICHHARDT C., Phys. Rev. Lett., 95 (2005) 088001.
- [11] CANDELIER R. and DAUCHOT O., Phys. Rev. E, 81 (2010) 011304.

- [12] KOLB E., CIXOUS P., GAUDOUEN N. and DARNIGE T., Phys. Rev. E, 87 (2013) 032207.
- [13] GRUBER M., ABADE G. C., PUERTAS A. M. and FUCHS M., Phys. Rev. E, 94 (2016) 042602.
- [14] ŞENBIL N., GRUBER M., ZHANG C., FUCHS M. and SCHEFFOLD F., Phys. Rev. Lett., 122 (2019) 108002.
- [15] GRUBER M., PUERTAS A. M. and FUCHS M., Phys. Rev. E, 101 (2020) 012612.
- [16] REICHHARDT C. and REICHHARDT C. J. O., Phys. Rev. E, 91 (2015) 032313.
- [17] WULFERT R., SEIFERT U. and SPECK T., Soft Matter, 13 (2017) 9093.
- [18] DULLENS R. P. A. and BECHINGER C., Phys. Rev. Lett., 107 (2011) 138301.
- [19] Wang H., Mohorič T., Zhang X., Dobnikar J. and Horbach J., Soft Matter, 15 (2019) 4437.
- [20] ABAURREA-VELASCO C., LOZANO C., BECHINGER C. and DE GRAAF J., Phys. Rev. Lett., 125 (2020) 258002.
- [21] AVRON J. E., SEILER R. and ZOGRAF P. G., Phys. Rev. Lett., 75 (1995) 697.
- [22] AVRON J. E., J. Stat. Phys., 92 (1998) 543.
- [23] LIFSHITZ E. M. and PITAEVSKI L. P., Physical Kinetics (Pergamon Press) 1981.
- [24] WIEGMANN P. and ABANOV A. G., Phys. Rev. Lett., 113 (2014) 034501.
- [25] ABANOV A. G., CAN T., GANESHAN S. and MONTEIRO G. M., Phys. Rev. Fluids, 5 (2020) 104802.
- [26] Banerjee D., Souslov A., Abanov A. G. and Vitelli V., *Nature Commun.*, 8 (2017) 1573.
- [27] SONI V., BILILIGN E. S., MAGKIRIADOU S., SACANNA S., BARTOLO D., SHELLEY M. J. and IRVINE W. T. M., Nature Phys., 15 (2019) 1188.
- [28] SOUSLOV A., DASBISWAS K., FRUCHART M., VAIKUN-TANATHAN S. and VITELLI V., Phys. Rev. Lett., 122 (2019) 128001.
- [29] HARGUS C., KLYMKO K., EPSTEIN J. M. and MAN-DADAPU K. K., J. Chem. Phys., 152 (2020) 201102.
- [30] HOSAKA Y., KOMURA S. and ANDELMAN D., Phys. Rev. E, 103 (2021) 042610.
- [31] MARKOVICH T. and LUBENSKY T. C., arXiv e-prints, () arXiv:2006.05662.
- [32] SCHEIBNER C., SOUSLOV A., BANERJEE D., SUROWKA P., IRVINE W. T. M. and VITELLI V., Nature Phys., 16 (2020) 475.
- [33] REICHHARDT C. J. O. and REICHHARDT C., *Nature*, **592** (2021) 355.
- [34] FRUCHART M., HANAI R., LITTLEWOOD P. B. and VITELLI V., *Nature*, **592** (2021) 363.
- [35] MÜHLBAUER S., BINZ B., JONIETZ F., PFLEIDERER C., ROSCH A., NEUBAUER A., GEORGII R. and BÖNI P., Science, 323 (2009) 915.
- [36] Yu X. Z., Onose Y., Kanazawa N., Park J. H., Han J. H., Matsui Y., Nagaosa N. and Tokura Y., *Nature* (*London*), 465 (2010) 901.
- [37] NAGAOSA N. and TOKURA Y., Nature Nanotechnol., 8 (2013) 899.
- [38] EVERSCHOR-SITTE K. and SITTE M., J. Appl. Phys., 115 (2014) 172602.
- [39] REICHHARDT C., REICHHARDT C. J. O. and MILOSEVIC M. V., arXiv e-prints, () arXiv:2102.10464.
- [40] LIN S.-Z., REICHHARDT C., BATISTA C. D. and SAXENA A., Phys. Rev. B, 87 (2013) 214419.

- [41] JIANG W., ZHANG X., YU G., ZHANG W., WANG X., JUNGFLEISCH M. B., PEARSON J. E., CHENG X., HEINONEN O., WANG K. L., ZHOU Y., HOFFMANN A. and TE VELTHUIS S. G. E., *Nature Phys.*, **13** (2017) 162.
- [42] LITZIUS K., LEMESH I., KRÜGER B., BASSIRIAN P., CARETTA L., RICHTER K., BÜTTNER F., SATO K., TRETIAKOV O. A., FÖRSTER J., REEVE R. M., WEIGAND M., BYKOVA L., STOLL H., SCHÜTZ G., BEACH G. S. D. and KLÄUI M., *Nature Phys.*, **13** (2017) 170.
- [43] REICHHARDT C. and REICHHARDT C. J. O., Nature Commun., 11 (2020) 738.
- [44] JUGE R., JE S.-G., CHAVES D. D. S., BUDA-PREJBEANU L. D., PEÑA GARCIA J., NATH J., MIRON I. M., RANA K. G., ABALLE L., FOERSTER M., GENUZIO F., MENTEŞ T. O., LOCATELLI A., MACCHEROZZI F., DHESI S. S., BELMEGUENAI M., ROUSSIGNÉ Y., AUFFRET S., PIZZINI S., GAUDIN G., VOGEL J. and BOULLE O., *Phys. Rev. Applied*, **12** (2019) 044007.
- [45] ZEISSLER K., FINIZIO S., BARTON C., HUXTABLE A. J., MASSEY J., RAABE J., SADOVNIKOV A. V., NIKITOV S. A., BREARTON R., HESJEDAL T., VAN DER LAAN G., ROSAMOND M. C., LINFIELD E. H., BURNELL G. and MARROWS C. H., Nature Commun., 11 (2020) 428.
- [46] REICHHARDT C., RAY D. and REICHHARDT C. J. O., Phys. Rev. Lett., 114 (2015) 217202.
- [47] IWASAKI J., KOSHIBAE W. and NAGAOSA N., Nano Lett., 14 (2014) 4432.
- [48] CASTELL-QUERALT J., GONZALEZ-GOMEZ L., DEL-VALLE N., SANCHEZ A. and NAVAU C., Nanoscale, 11 (2019) 12589.
- [49] REICHHARDT C. and REICHHARDT C. J. O., Phys. Rev. E, 100 (2019) 012604.